Schweizerischer Erdbebendienst
Service Sismologique Suisse
Servizio Sismico Svizzero
Swiss Seismological Service

ETH
Eidgenössische Technische Hochschule Zürich
Swiss Federal Institute of Technology Zurich

SITE CHARACTERIZATION REPORT

SWYZ: Schwyz (SZ)

Francesco Panzera, Manuel Hobiger, Donat Fäh

Last Modification: 2nd December, 2019

Schweizerischer Erdbebendienst (SED)
Service Sismologique Suisse
Servizio Sismico Svizzero
Servizi da Terratrembels Svizzer
ETH Zürich
Sonneggstrasse 5
8092 Zürich
Schweiz
francesco.panzera@sed.ethz.ch

Contents

Summary

Schwyz (SZ), located in central Switzerland, was selected as site for the installation of a new station, called SWYZ, as part of the renewal project of the Swiss Strong Motion Network (SSMNet). In order to better assess the local subsurface, we performed site characterization measurements with different techniques. The results of the horizontal-to-vertical spectral ratio (H/V), show curves with a clear peak fundamental peak between 1.2 and 1.4 Hz. The slight variability in the secondary frequency peak (from 7.8 to 19.0 Hz) is related to the presence of a variable thickness cover of infill in the area of the seismic station.

The inversion of the passive seismic array measurements allows determining a main possible discontinuity linked to the bedrock at about 300-320 m, with velocity reaching 3000 m/s. Above the bedrock, two main discontinuities can be identified. The first at about 20-30 m and the second one at about 100 m. The first layer has a velocity increasing with depth from 150 to 730 m/s, whereas the second layer is characterized by a velocity of about 1500 m/s. The V_{S30} value of the site is about 551 m/s, corresponding to soil class B in EC8 and in SIA261. The theoretical shear-wave transfer functions from the retrieved V_S profiles predict an amplification peak at about 1.2 Hz, in good agreement with the fundamental H/V frequency of the site.

1 Introduction

The station SWYZ is part of the Swiss Strong Motion Network (SSMNet). The station has been installed on 19 July 2018 in the framework of the second phase of the Swiss Strong Motion Network (SSMNet) renewal project (Fig. 1). In order to better characterize the underground of the station, we performed passive array measurements.
The site is of interest because it is located in a populated area in central-eastern Switzerland at the border between the Molasse basin and the Helvetic nappes. Its geographical location improves the network coverage of the area.
The measurement campaign was carried out on 11 October 2019 in order to characterize the soil column in terms of fundamental frequency and shear wave velocity.

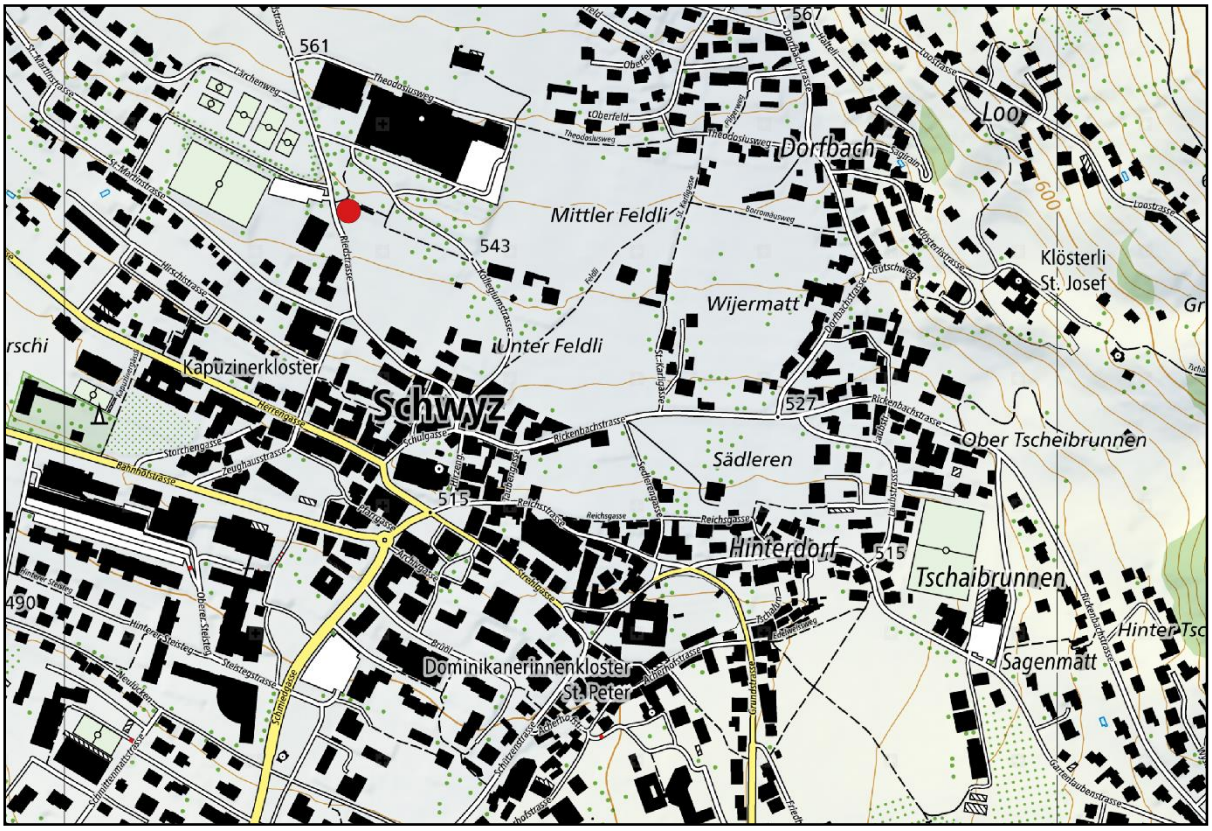

Figure 1: Map showing the location of the strong motion station (red circle) in Schwyz. © 2019 swisstopo (JD100042)

2 Geological setting

A geological map of the surroundings of the site in Schwyz is shown in Fig. 2, together with the stations of the passive array measurements. All the sixteen stations of the passive array measurement lie on river gravel deposit. The seismic station SWYZ is located on the same formation.

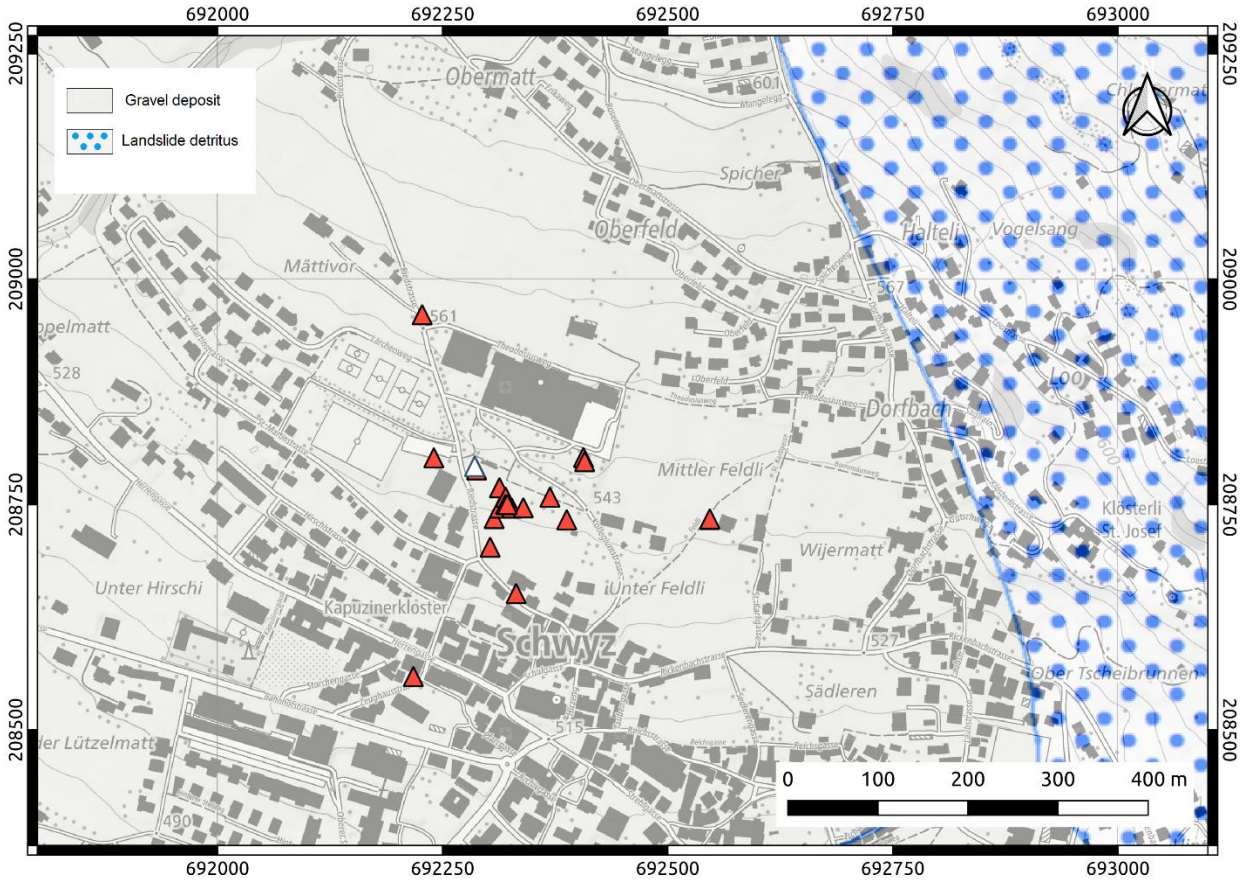

Figure 2: Geological map of the SWYZ seismic station area. The stations of the passive array recordings are indicated by red triangles, whereas the SWYZ strong motion station position is shown by a white triangle. © 2019 swisstopo (JD100042)

3 Site characterization measurements

3.1 Data set

To characterize the deeper underground structure around the seismic station, we performed passive seismic measurements in October 2019, together with a H/V measurement at the location of SWYZ station (Fig. 3).

A single array of 16 stations was installed (Fig. 4). The stations were planned to be located on five rings of different radii around a central station. The three inner rings were planned in regular forms with angular distances of 120 between the different stations on the ring. These three rings had radii of 8, 20 and 50 m, respectively. The inner ring had the central station facing south-east from the central station (SWY066). The second and third rings were rotated by 20 degrees with respect to the first and second rings, respectively. The fourth ring was planned to have a distance of 100 m from the central station. The stations of the fifth ring were placed at distance of about 228 m from the array center. The minimum and maximum interstation distances in the finally installed array were 8.0 and 228 m, respectively.

Each station consisted of a Lennartz 5s sensor connected to a Centaur digitizer, with the exception of four stations in the central part which had two sensors connected to the same digitizer. The station names of the array are composed of "SWY" followed by a three-digit number between 42 and 49, 52 and 55, 62, 66, 73 and 74 (corresponding to the Centaur digitizer serial number for numbers lower than 60 and serial number plus 20 for higher numbers). The array recording time was 150 minutes (10200 s). The station locations were measured by a differential GPS system (Leica Viva GS10) which was set up to measure with a precision better than 3 cm.

Figure 3: Seismic station installation example for the measurements in Schwyz.

Figure 4: Layout of the array measurement in Schwyz. The locations of the stations for the passive seismic measurement are indicated by the red triangles. The white triangle indicates the seismic station site. © 2019 swisstopo (JD100042)

3.2 H/V and RayDec ellipticity curves

Figure 5 shows the H/V curves determined with the time-frequency analysis method (Fäh et al., 2009) for all stations of the passive array. The H/V curves are quite homogeneous and show a similar pattern up to 5.0 Hz, with a fundamental frequency of about 1.25 Hz. Above this frequency value most of the curves are characterized by peaks between 8.0 and about 18.0 Hz. This behavior indicates the presence of a thin infill deposits in the area, with variable thickness.

The RayDec technique (Hobiger et al., 2009) is meant to eliminate the contributions of other wave types than Rayleigh waves and give a better estimate of the ellipticity than the classical H/V technique. The RayDec ellipticity curves for all stations of the array measurements are shown in Figure 5. The RayDec curves of the different stations are similar to the one obtained through H/V.

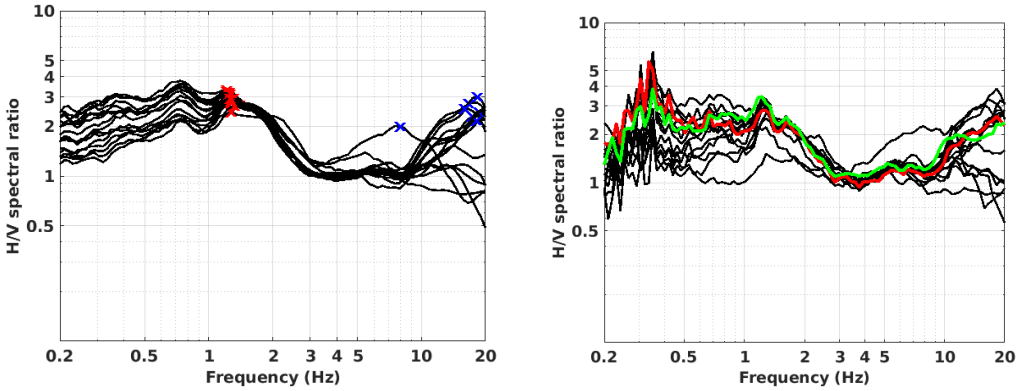

Figure 5: Left: H/V curves of the different stations of the array measurements in Schwyz with picked fundamental frequency (red cross) and secondary peak (blue cross). Right: RayDec ellipticities for all stations of the array. The curve of SWY066, the array center is highlighted in red, whereas the curve SWY042, linked to the measurement nearby the station is highlighted in green.

3.3 Polarization measurements

The polarization analysis was performed according to Burjánek et al. (2010) and Burjánek et al. (2012). The results for all stations of the array are similar. Only the results for SWY066, at the array center (see location in Fig. 3), are shown in Fig. 6. The results show that the ground motion is almost linear and horizontally polarized around the H/V peak. In the strike plot no marked polarization directions are present.

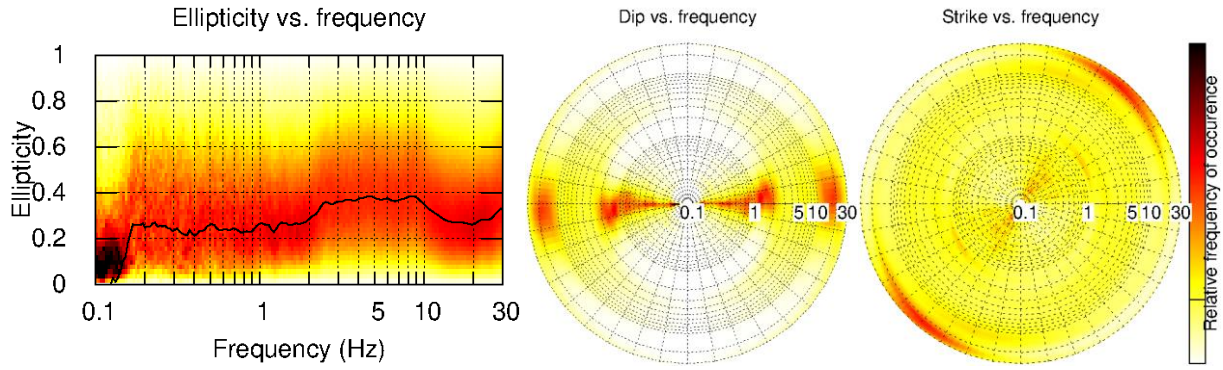

Figure 6: Polarization analysis of station SWY066.

3.4 3-component high-resolution FK

The results of the 3-component high-resolution FK analysis (Poggi and Fäh, 2010) are shown in Fig. 7. The results on the transverse component show the dispersion curve (DC) of one mode of Love waves from 2.6 to 12.0 Hz. On the radial component we identified a mode in the frequency range 3.4 to 16.0 Hz. On the vertical component two modes were picked, from 3.3 to 13.0 Hz and from 9.6 to 18.5 Hz. The corresponding ellipticity curves of the radial and vertical components are clearly identified in the corresponding frequency ranges. In particular, the radial component shows an ascendant ellipticity amplitude, whereas the transversal one is almost flat.

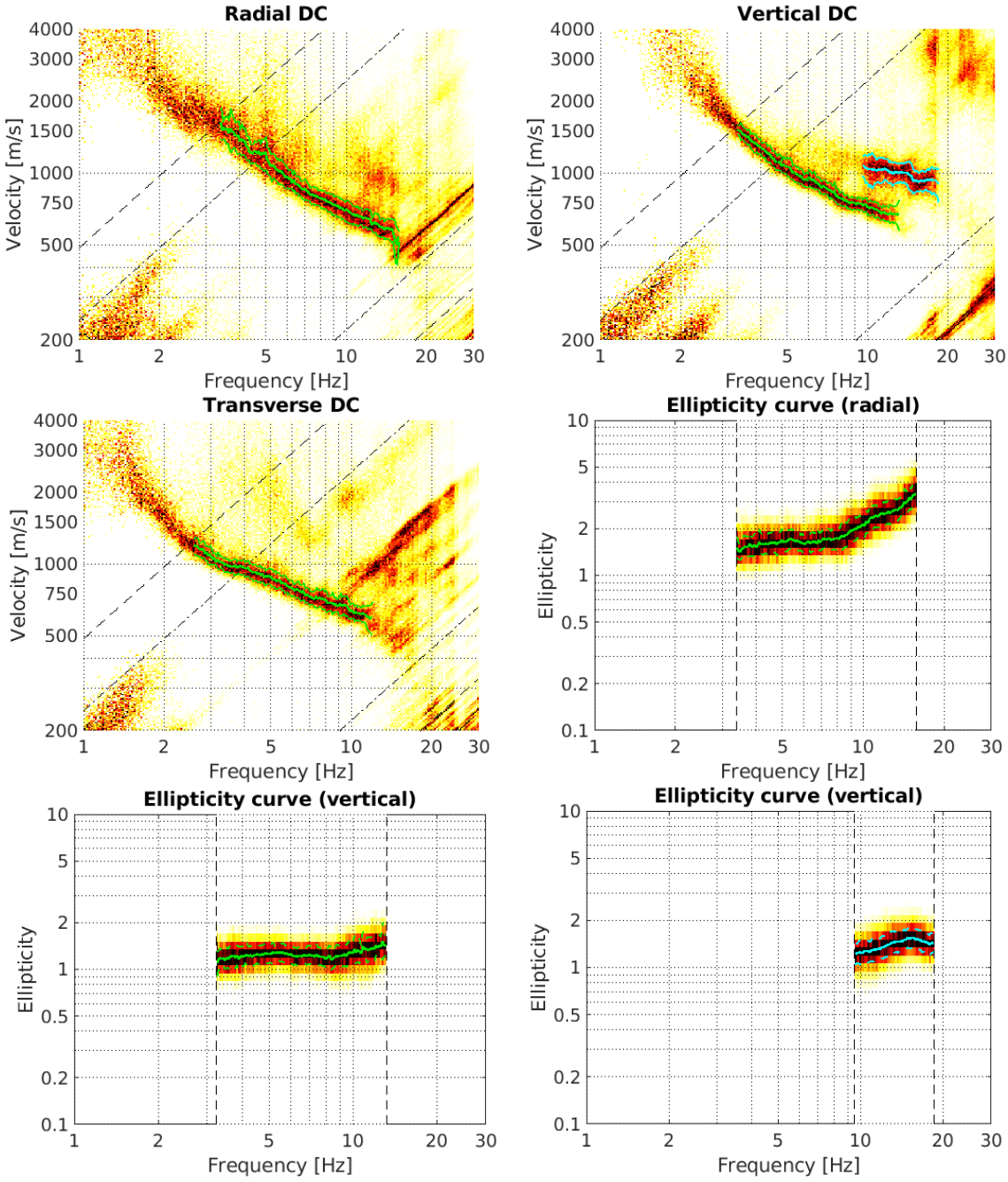

Figure 7: Dispersion and ellipticity curves for the transverse, radial and vertical components obtained with the 3-component HRFK algorithm (Poggi and Fäh, 2010). The dashed and dotted black lines are the array resolution limits. The solid and dashed green lines represent the data picking, where the central line indicates the best value and the two outer lines the standard deviation for the fundamental and first higher mode, respectively.

3.5 WaveDec

The results of the WaveDec code (Maranò et al., 2012) processing are shown in Fig. 8. This technique estimates the properties of single or multiple waves simultaneously with a maximum likelihood approach. In order to get good results, the parameter γ must be tuned to modify the sharpness of the wave property estimation between purely maximum likelihood estimation and a Bayesian Information Criterion. Here, a value of $\gamma = 0.2$ was used, corresponding to a mostly maximum likelihood estimation.

The Love wave dispersion curve is clearly retrieved between about 2.5 and 16.6 Hz. The Rayleigh wave dispersion curve can be picked between 3.2 Hz and 16.6 Hz. The ellipticity angle for the picked Rayleigh wave dispersion curve is negative throughout all the considered frequency range, indicating a retrograde particle motion. The ellipticity angle goes towards -90° above 15 Hz, which would be compatible with an ellipticity ratio singularity and a change of the particle motion to prograde. The ellipticity curve is characterized by an ascendant ellipticity amplitude.

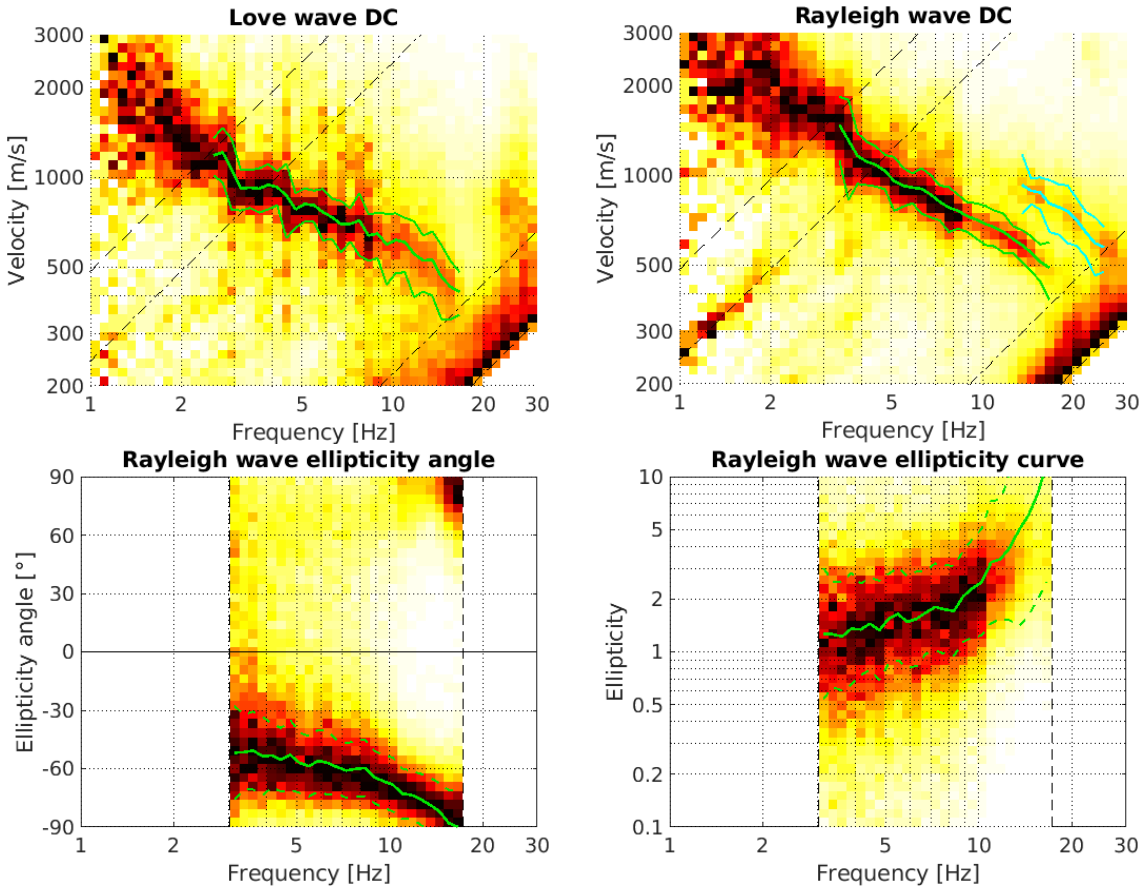

Figure 8: Dispersion curves for Love and Rayleigh waves and ellipticity curve for Rayleigh waves as obtained with WaveDec (Maranò et al., 2012). The solid and dashed green lines represent the data picking, where the central line indicates the best value and the two outer lines the standard deviation

3.6 Summary

Figure 9 gives an overview of the dispersion and ellipticity curves determined by the different methods. For Love waves, WaveDec produces a dispersion curve that is similar to HRFK, although with slightly lower phase velocities. For the Rayleigh waves, there is also a good agreement between the two different methods for the fundamental mode, but no higher modes are observed in WaveDec. Moreover, from the radial component of HRFK we can observe the DC behavior at frequency higher than 13.0 Hz.

The ellipticity curves retrieved using the different methods are quite similar. The RayDec curve has a peak at about 18.0 Hz and the WaveDec curve is defined only for the ascendant flank of the secondary frequency peak observed in the H/V. The ellipticity retrieved from the HRFK radial component has the same shape of RayDec and WaveDec curves. Finally, the ellipticity obtained from HRFK vertical component has tends to slightly increase its amplitude from 3.5 to about 13.0 Hz, conversely the shape of the HRFK ellipticity for the first higher mode depicts a peak at about 15.0 Hz.

From the ellipticity angle is possible to observe the change of particle motion from retrograde to prograde at about 18.0 Hz (Fig. 8).

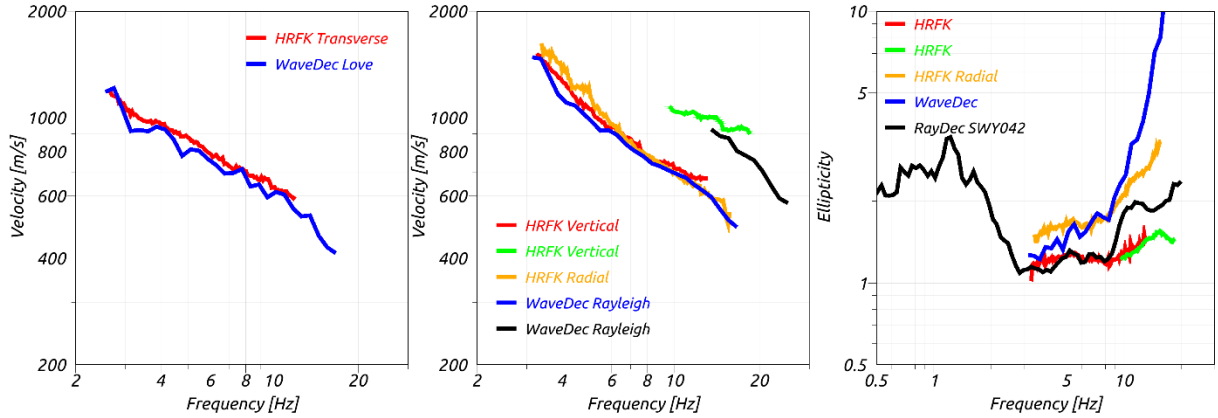

Figure 9: Comparison between the computed dispersion curves and ellipticity curves. The RayDec curve is related to the measurement point SWY042.

4 Data inversion

4.1 Inversion targets

We performed several inversions using as much information as possible, resorting to different parts of the picked dispersion and ellipticity curves. The details of the inversion target are indicated in Table 1 and the corresponding curves are shown in Fig. 10.

In the inversion process, we used the curve obtained with WaveDec as Love wave fundamental mode, because it covers a larger frequency range up to 16.6 Hz with respect to HRFK. Also for the Rayleigh wave dispersion curve we used WaveDec results, distinguishing a fundamental mode and a first higher mode. The inversion process was also performed using the RayDec ellipticity from station SWY042.

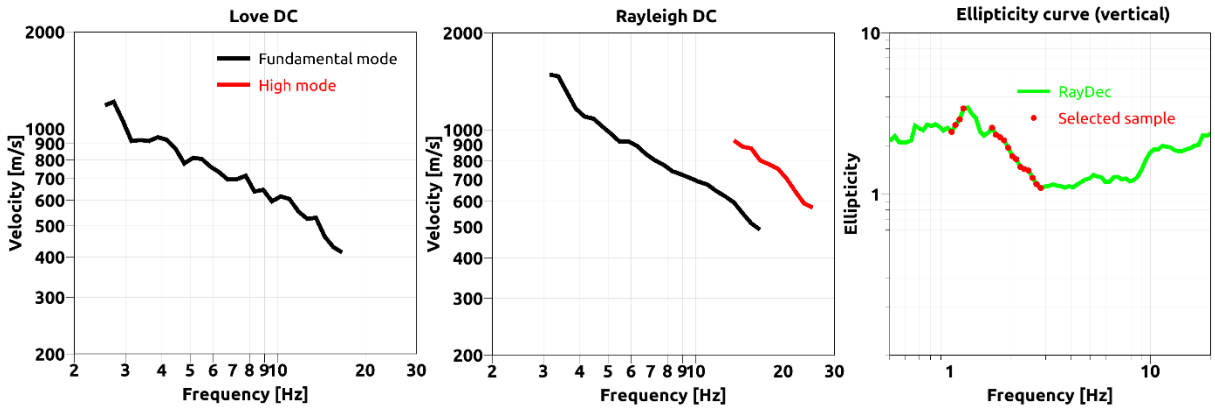

Figure 10: Overview of the dispersion curves used as target for the different inversions.

Table 1: List of the curves used as target in the inversion.

Method	Wave type	Mode	Curve type	Frequency range [Hz]
WaveDec	Love	fundamental	dispersion	2.5-16.6
WaveDec	Rayleigh	fundamental	dispersion	3.4-16.6
WaveDec	Rayleigh	first	dispersion	13.5-25.2
RayDec (SWY042)	Rayleigh	fundamental	ellipticity	1.00-1.23
RayDec (SWY042)	Rayleigh	fundamental	ellipticity	1.60-2.83

4.2 Inversion parameterization

For the inversion, six different parameterizations were tested. The first five involve free values of thickness and velocities for the different layers, ranging from four to eight layers (including half-space). The last parameterization had fixed layer thicknesses and consists of 17 layers in total, with the deepest interface at 300m depth.

The S- and P-wave velocities are allowed to range from 100 to 4000 m/s and from 200 to 5000 m/s, respectively. The deepest layer interfaces were allowed to range to a depth of 400 m for all parameterizations. The density was fixed to 2300 kg/m^3 for the bedrock layer and to 2000 kg/m^3 for all other layers.

4.3 Inversion results

We performed a total of 7 inversions with different parameterizations (see Table 2) using the Dinver routine (http://www.geopsy.org/). Each inversion run produced 200000 total models in order to assure a good convergence of the solution. The results of these inversions are shown in Figs 11 – 16.

Table 2: List of inversions

Inversion	Number of layers	Number of models	Minimum misfit
SWYZ4l	4	200000	0.527197
SWYZ 5l	5	200000	0.480737
SWYZ 6l	6	200000	0.515980
SWYZ 7l	7	200000	0.503902
SWYZ 8l	8	200000	0.517896
SWYZ fix	15	200000	0.468850

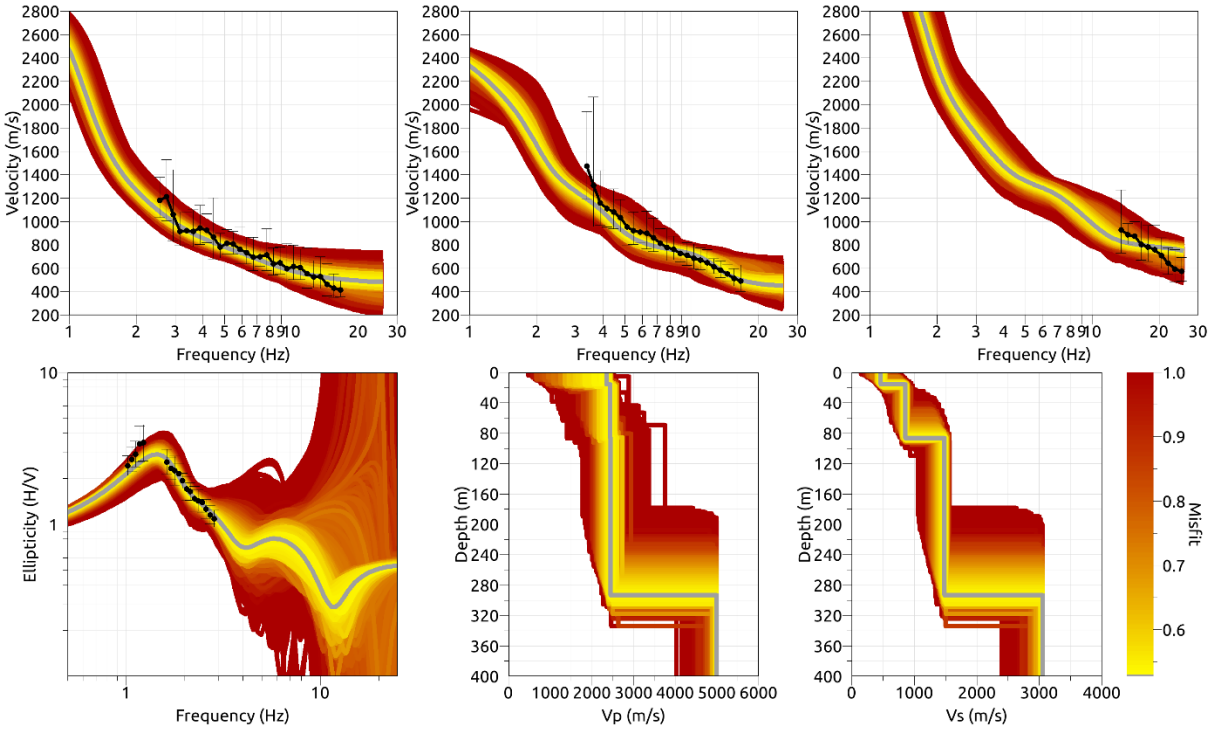

Figure 11: Inversion SWYZ4l. Top line: Dispersion curves for the Love wave fundamental mode (left), the Rayleigh wave fundamental (center) and first higher mode (right). Bottom line: Ellipticity curve (left), P-wave velocity profiles (center) and S-wave velocity profiles (right). The black dots indicate the data points used for the inversion, the gray line indicates the best-fitting model.

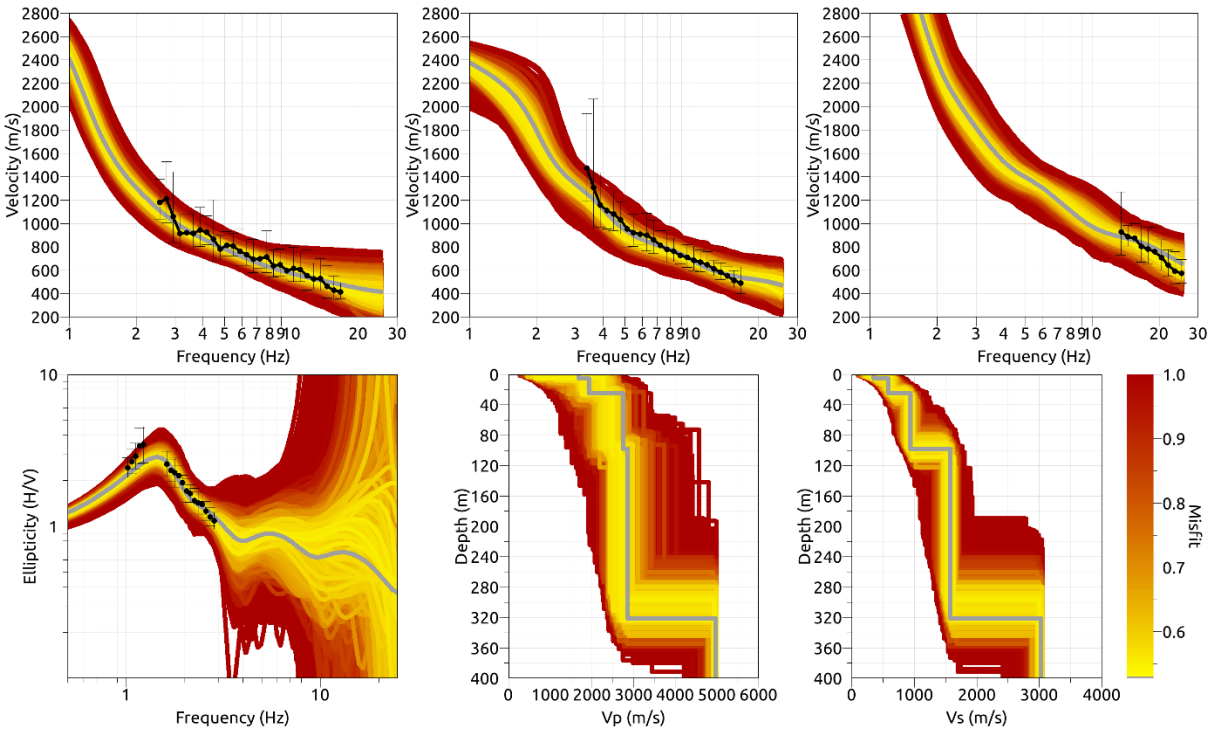

Figure 12: Inversion SWYZ5l. Top line: Dispersion curves for the Love wave fundamental mode (left), the Rayleigh wave fundamental (center) and first higher mode (right). Bottom line: Ellipticity curve (left), P-wave velocity profiles (center) and S-wave velocity profiles (right). The black dots indicate the data points used for the inversion, the gray line indicates the best-fitting model.

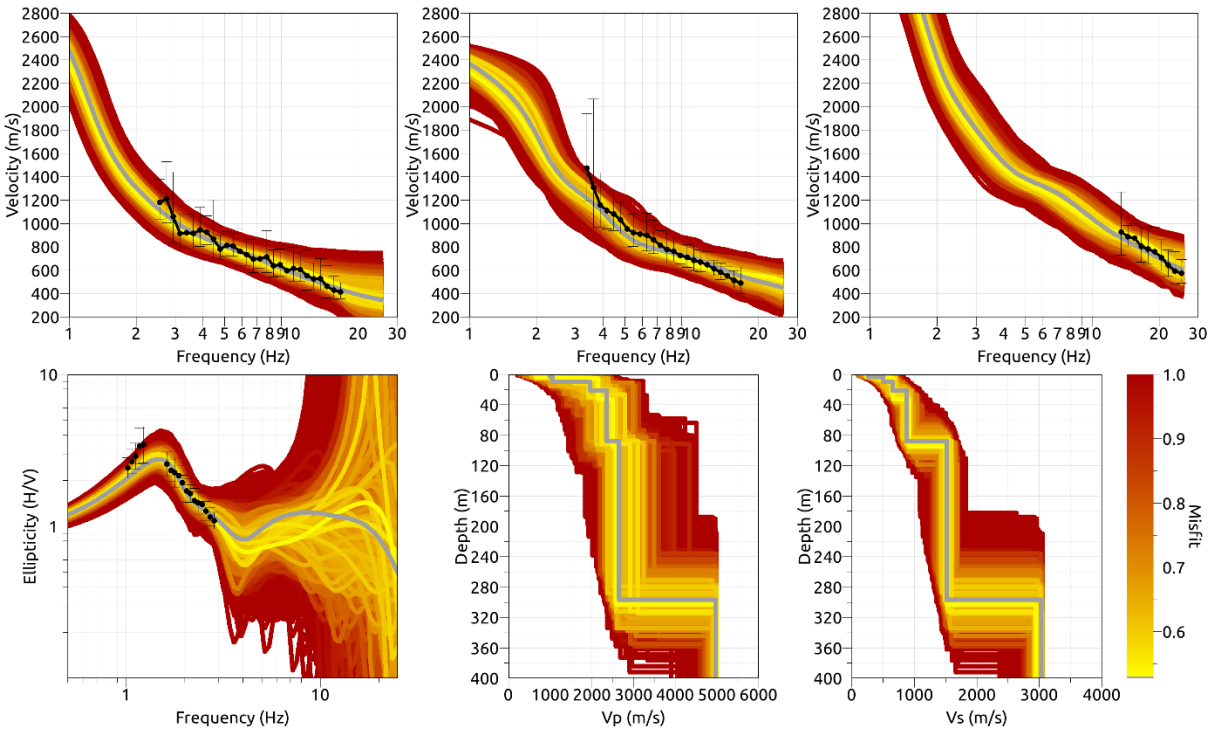

Figure 13: Inversion SWYZ6l. Top line: Dispersion curves for the Love wave fundamental mode (left), the Rayleigh wave fundamental (center) and first higher mode (right). Bottom line: Ellipticity curve (left), P-wave velocity profiles (center) and S-wave velocity profiles (right). The black dots indicate the data points used for the inversion, the gray line indicates the best-fitting model.

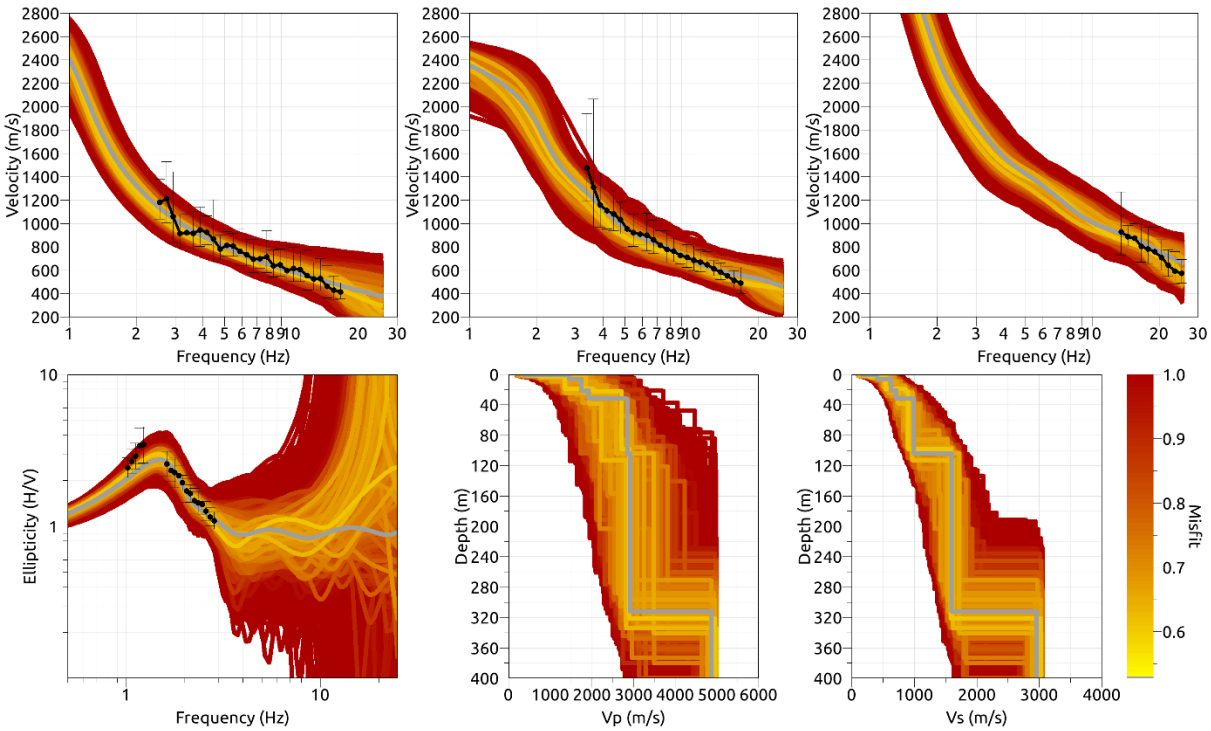

Figure 14: Inversion SWYZ7l. Top line: Dispersion curves for the Love wave fundamental mode (left), the Rayleigh wave fundamental (center) and first higher mode (right). Bottom line: Ellipticity curve (left), P-wave velocity profiles (center) and S-wave velocity profiles (right). The black dots indicate the data points used for the inversion, the gray line indicates the best-fitting model.

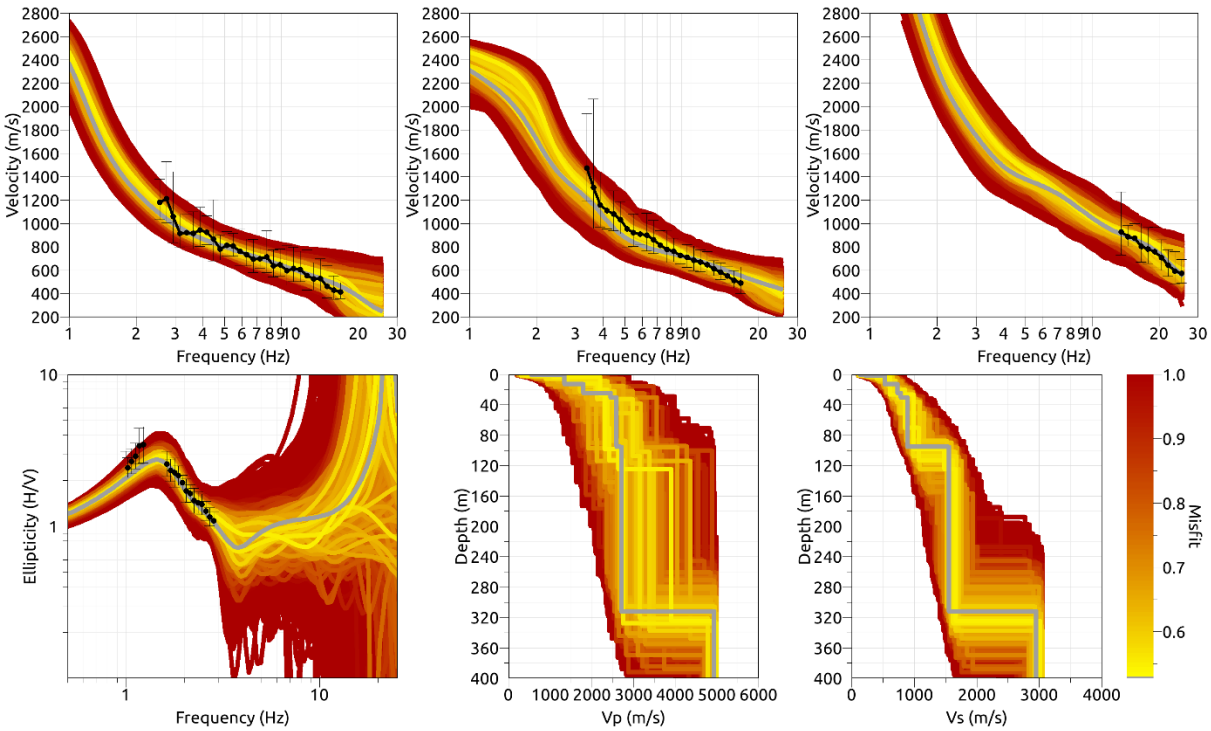

Figure 15: Inversion SWYZ8l. Top line: Dispersion curves for the Love wave fundamental mode (left), the Rayleigh wave fundamental (center) and first higher mode (right). Bottom line: Ellipticity curve (left), P-wave velocity profiles (center) and S-wave velocity profiles (right). The black dots indicate the data points used for the inversion, the gray line indicates the best-fitting model.

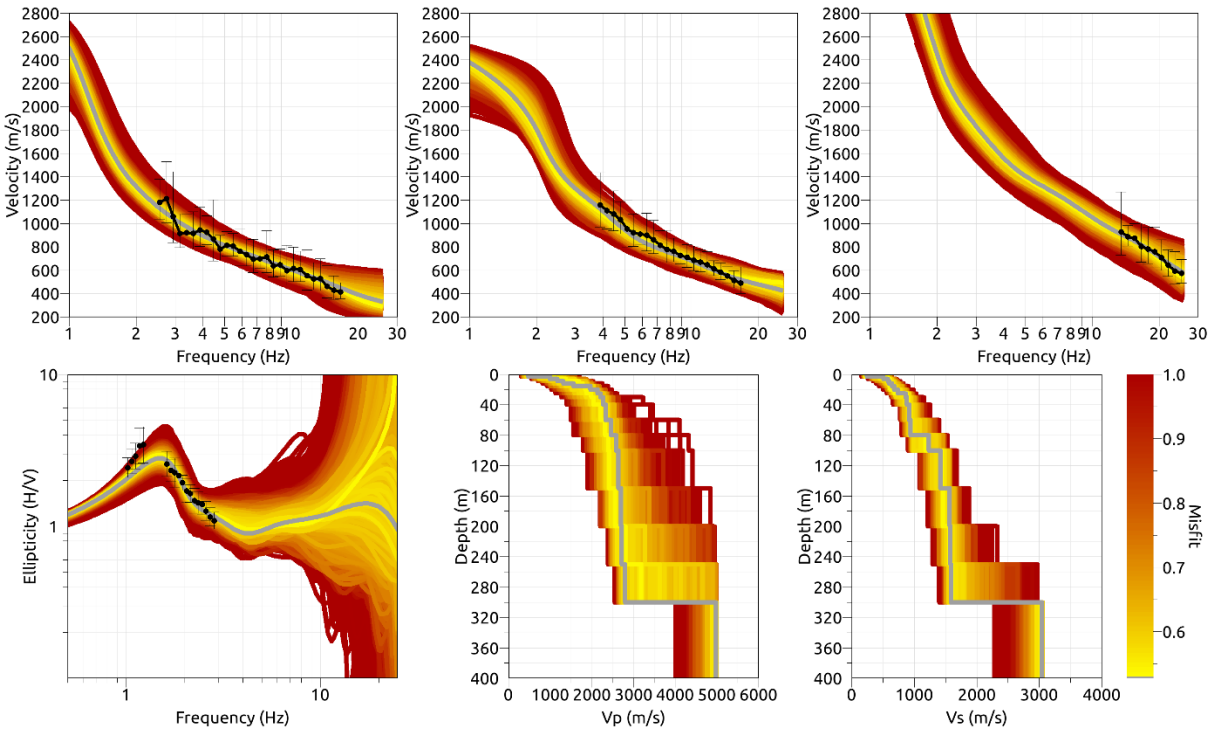

Figure 16: Inversion SWYZfix. Top line: Dispersion curves for the Love wave fundamental mode (left), the Rayleigh wave fundamental (center) and first higher mode (right). Bottom line: Ellipticity curve (left), P-wave velocity profiles (center) and S-wave velocity profiles (right). The black dots indicate the data points used for the inversion, the gray line indicates the best-fitting model.

4.4 Discussion of the inversion results

The best-fitting models from each inversion are shown in Fig. 17. There are several main features that all models share. The seismic bedrock is found at depths between 300 and 320 m, with a shear wave velocity of about 3000 m/s. Above the bedrock, two main discontinuities are visible. The first at about 20-30 m and the second at about 100 m. The first layer has a velocity increasing with depth from 150 to 730 m/s, whereas the second layer is characterized by a velocity of about 1500 m/s. The velocity profiles resulting from the different inversions have V_{S30} between 538.9 and 569.7 m/s, with an average value of 561.1 ± 19.7 m/s.

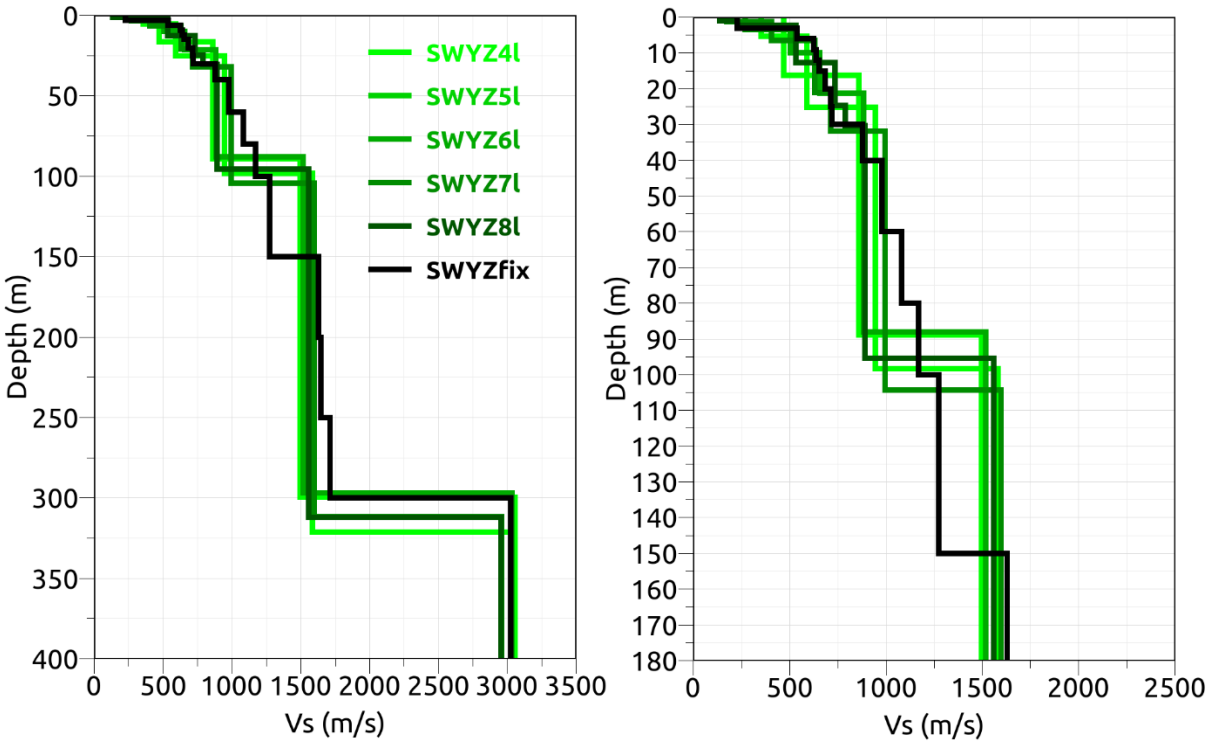

Figure 17: Overview of the best shear-wave velocity profiles of the different inversions (left) and zoom on the upper 180 m of the inversion profiles.

5 Further results from the inverted profiles

5.1 SH transfer function

In Figure 18, the average theoretical shear-wave transfer function from the obtained models is shown. In this case, the models are predicting an amplification up to a factor of 2.0 at about 1.5 Hz. The present (01.12.2019) empirical amplification is not stable considering the low number of earthquake used for its computation, but a quite good agreement is observed, especially at high frequency. As soon as the station has recorded a sufficient number of earthquakes the comparison will be repeated.

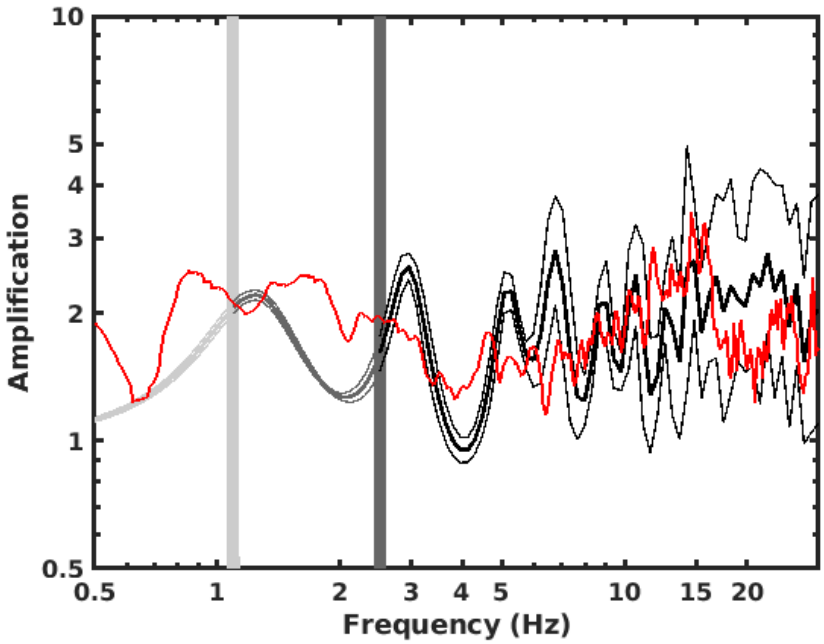

Figure 18: Modeled amplification function for the best models of the six inversions (black and gray lines). Red curve is the empirical amplification function at the SWYZ station.

5.2 Quarter-wavelength representation

The quarter-wavelength velocity approach (Joyner et al., 1981) provides, for a given frequency, the average velocity at a depth corresponding to 1/4 of the wavelength of interest (Fig. 19). The results using this proxy, considering frequency limits of the experimental data of 2.5 to 25.0 Hz for the dispersion curves, is well constrained above 30 m. The quarter wavelength impedance-contrast introduced by Poggi et al. (2012) is also displayed in the figure. It corresponds to the ratio between two quarter-wavelength average velocities, respectively from the top and the bottom part of the velocity profile, at a given frequency.

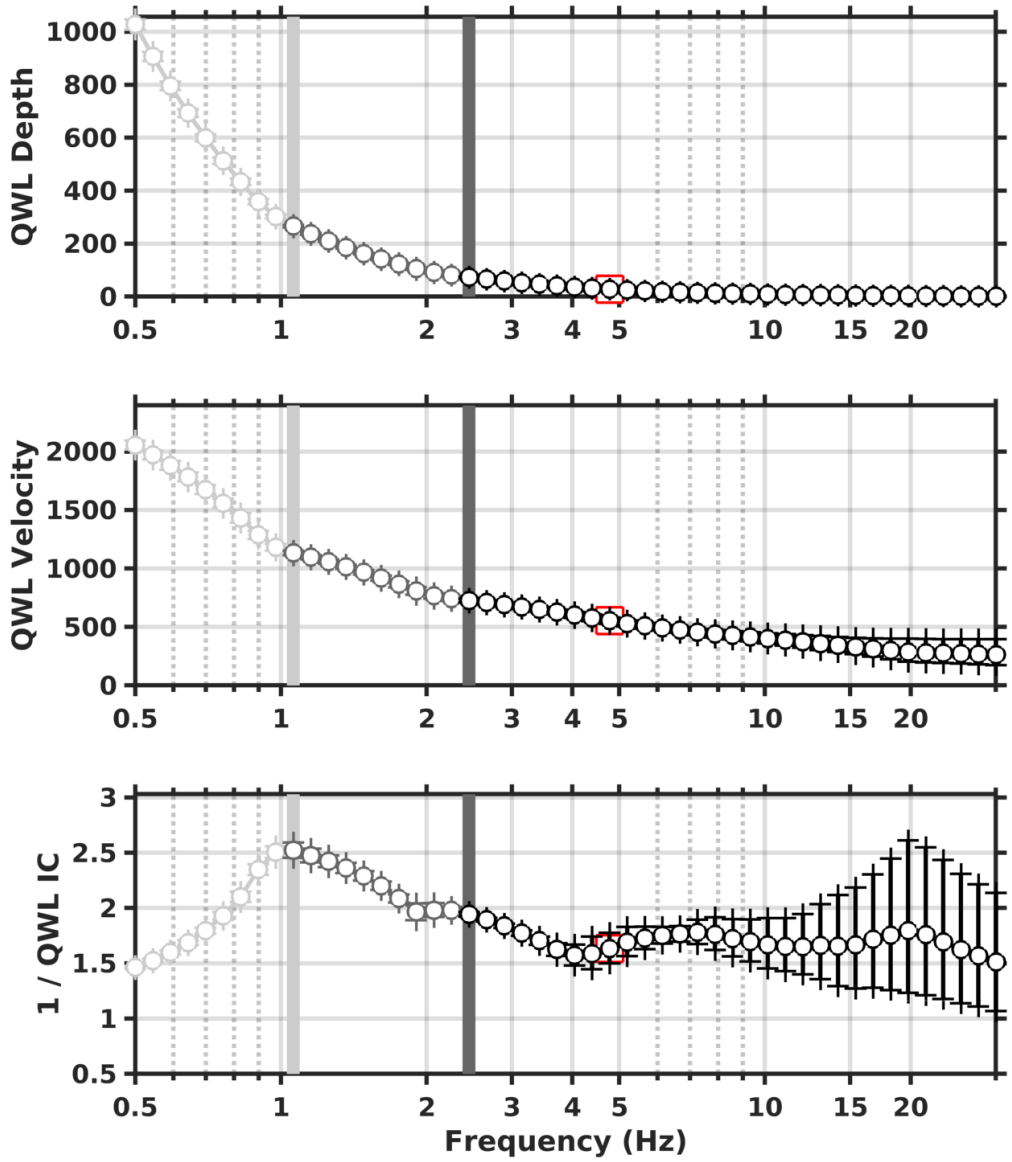

Figure 19: Quarter wavelength representation of the velocity profiles for the best models of the inversions (top: depth, center: velocity, bottom: inverse of the impedance contrast). The grey light bar shows ellipticity lower frequency value, dark grey bar indicates lower frequency value obtained with dispersion curves and red square corresponds to f_{30} (frequency related to the depth of 30 m).

6 Discussion and conclusions

The H/V analysis points out that the fundamental peak observed at the different stations is quite stable and can be explained with a sub-horizontal bedrock below the seismic station site.
The inversion of the passive seismic array measurements yields a velocity profile with 3 main interface at about 20-30 m, 100 m and 300 m. In particular, the soft layer has a velocity increasing with depth from 150 to 730 m/s, a second layer is then present with a velocity of about 1500 m/s. The bedrock is reached at about 300 m, with a velocity of about 3000 m/s. The V_{S30} value of the site is determined as about 561 m/s, corresponding to soil class B in EC8 and in SIA261 classifications.
The theoretical shear-wave transfer function predicts an amplification factor of around 2 at about 1.2 Hz, in quite good agreement with the 1.2-1.4 Hz fundamental frequency of the site where the strong motion station is installed. The comparison was also made with amplification observations at this station, showing a quite good agreement, especially at high frequency.

Acknowledgements

The authors thank Paulina Janusz for her help during the measurements.

References

Burjánek, J., Gassner-Stamm, G., Poggi, V., Moore, J. R., and Fäh, D. (2010). Ambient vibration analysis of an unstable mountain slope. Geophys. J. Int., 180:820–828.

Burjánek, J., Moore, J. R., Molina, F. X. Y., and Fäh, D. (2012). Instrumental evidence of normal mode rock slope vibration. Geophys. J. Int., 188:559–569.

Fäh, D., Gardini, D., et al. (2003). Earthquake Cataloque of Switzerland (ECOS) and the related macroseismic database. Eclogae geol. Helv. 96.

Fäh, D., Wathelet, M., Kristekova, M., Havenith, H., Endrun, B., Stamm, G., Poggi, V., Burjanek, J., and Cornou, C. (2009). Using ellipticity information for site characterisation. NERIES deliverable JRA4 D4, available at http://www.neries-eu.org.

Fritsche, S., Fäh, D., Gisler, M., and Giardini, D. (2006). Reconstructing the damage field of the 1855 earthquake inSwitzerland: historical investigations on a well-documented event Geophys. J. Int. (2006)166, 719–731

Hobiger, M., Bard, P.-Y., Cornou, C., and Le Bihan, N. (2009). Single station determination of Rayleigh wave ellipticity by using the random decrement technique (RayDec). Geophys. Res. Lett., 36.

Maranò, S., Reller, C., Loeliger, H.-A., and Fäh, D. (2012). Seismic waves estimation and wavefield decomposition: Application to ambient vibrations. Geophys. J. Int., 191:175–188.

Poggi, V. and Fäh, D. (2010). Estimating Rayleigh wave particle motion from three component array analysis of ambient vibrations. Geophys. J. Int., 180:251–267.

Poggi, V., Edwards, B., and Fäh, D. (2010). Characterizing the Vertical-to-Horizontal Ratio of Ground Motion at Soft-Sediment Sites. Bulletin of the Seismological Society of America, 102(6): 2741 2756.